minerals

Article

Effect of Basalt Fibers for Reinforcing Resin-Based Brake Composites

Xiaoguang Zhao [1], Jing Ouyang [1,2,3], Huaming Yang [1,2,3,*] and Qi Tan [4,*]

1 Department of Inorganic Materials, School of Minerals Processing and Bioengineering, Central South University, Changsha 410083, China; zhaoxiaoguang@csu.edu.cn (X.Z.); jingouyang@csu.edu.cn (J.O.)
2 Key Lab for Mineral Materials and Application of Hunan Province, Central South University, Changsha 410083, China
3 Key Lab of Clay Mineral Functional Materials in China Building Materials Industry, Central South University, Changsha 410083, China
4 Zhengzhou Institute of Multipurpose Utilization of Mineral Resources, Chinese Academy of Geological Sciences, Zhengzhou 450006, China
* Correspondence: hmyang@csu.edu.cn (H.Y.); tanqi@mail.cgs.gov.cn (Q.T.); Tel.: +86-731-88830549 (H.Y.); Fax: +86-731-88710804 (H.Y.)

Received: 15 April 2020; Accepted: 24 May 2020; Published: 27 May 2020

Abstract: Basalt fiber is an eco-friendly reinforcement fiber in fabricating polymer composites with high specific mechanical physicochemical, biodegradable, and wear resistant properties. This article firstly introduces the composition, morphology, functional group, and thermostability of basalt fibers. Subsequently, friction composites based on a newly designed formulation were fabricated with different content basalt fibers. According to the Chinese National Standard, the physical and mechanical properties and tribological performance of the friction composites were characterized and evaluated. Extension evaluation based on extenics theory was developed to evaluate the relationships between the coefficient of friction and content of basalt fiber. Furthermore, the possible mechanism of basalt fiber reinforced friction composites was proposed.

Keywords: basalt fiber; brake composites; mechanical and tribology performance; interfacial structure; mechanism

1. Introduction

Asbestos fiber has been a popular reinforcement used to fabricate brake pads over the past few decades, on account of its strength, resistance to heat and acid, chemical stability, and ease of machining [1]. However, it has already been confirmed that the micromolecule produced by the thermal decomposition of asbestos fiber is harmful to human health, as well as the environment [2,3]. In view of this, asbestos fiber has been forbidden by various countries. An increase in the demand of eco-friendly, natural fibers as reinforcement for the fabrication of resin-based friction materials can be seen globally in recent decades. In order to meet this need, many non-asbestos fibers have been developed, including mineral fiber [4–7], plant fiber [8–11], and artificial fiber such as Kevlar fiber [12], glass fiber [13,14], carbon fiber [15,16], etc. These fibers exhibit fairly good mechanical and friction properties. Although carbon fiber has been largely used in friction brake, especially in aircrafts and Formula 1 braking, high cost is still the main factor preventing its widespread usage. The others have some drawbacks more or less such as poor heat resistance, high cost, low-frequency braking noise, poor affinity with resin and other fillers, even harmful to human [7,17], these disadvantages severely limit their application in the automobile brake industry.

Basalt fibers have been extensively applied to military research for defense and aeronautical applications worldwide since their discovery [18,19]. In recent decades, basalt fibers have been used to fabricate light, high-end hybrid composite materials for infrastructural and civil applications due to their enhanced mechanical properties [20]. Based on their reliable structural properties, basalt fibers are a preferred choice of material in the construction industry. Branston et al. evaluated the relative merit of two types of basalt fibers (bundle dispersion fibers and minibars) in improving the mechanical capacity of concrete [21]. Both types of fibers could increase pre-cracking strength. However, only the latter could enhance the post-cracking behavior. Kabay et al. reported that basalt fibers could improve flexural strength, fracture energy and abrasion resistance of concretes, although the compressive strength of concrete would be reduced [22]. Basalt fiber as a strengthening material for concrete structures could not only enhance both the yielding and the ultimate strength of the beam specimen, but the strengthening didn't need to extend over the entire length of the flexural member [23]. Additionally, basalt fibers have received increasing attention as a novel type of reinforcement material in the fabrication of basalt-epoxy composites. Kim et al. developed a surface modified basalt fiber with low-temperature atmospheric oxygen plasma, and furthermore investigated the interlaminar fracture behavior of basalt fiber/epoxy woven composites [24]. They found the interlaminar fracture toughness of basalt fiber/epoxy woven composites was increased because the adhesive force between fiber/resin interfaces was enhanced by oxygen plasma treatment. Lee et al. explored the effects of surface treatment of a basalt fiber by chemical methods on the mechanical interfacial properties of basalt fibers reinforced epoxy composites [25]. Their results show the surface roughness of basalt fibers was increased, which further improved the interfacial bonding strength all in between basalt fibers and epoxy resin. A new perspective has arisen on filling fibers into a polymer matrix. Lopresto et al. investigated mechanical characteristic of basalt fiber reinforced plastic, and the results showed a high performance of the basalt material in terms of Young's modulus, compressive and bending strength, impact force, and energy [26]. In addition to these, basalt fiber could also be used in other applications, such as marine [27–29] and impact or ballistic resistance applications [30–33].

Generally speaking, when multiple combined foreign materials are embedded within an organic binder like resin, hybrid composite materials with synergistic effects are realized. By using this technique, novel types of basalt fiber reinforced friction materials are fabricated. Thirumalai et al. confirmed that basalt fibers in league with jute enhanced the tensile modulus and tensile strength of epoxy-based composites [34]. The basalt fiber length and the fiber content also have significant effects on the mechanical properties of friction composites. Amuthakkannan et al. revealed that 68% of fiber and 10 mm length of fiber exhibited better on flexural strength and tensile strength [35]. Basalt fibers also play roles in the tribological properties of friction composites. Three different fiber (flax fiber, basalt fiber, and flax/basalt composite fiber) reinforced hybrid phenolic composites were compared. The results indicated that basalt fiber had good thermal characteristics and bonding nature, which greatly improved the wear resistance of basalt fiber/phenolic resin composites, and the wear resistance of friction composites increased with the increase of basalt fiber content. Basalt fiber is a brake pad material with better properties than the other fiber reinforced composites [17,36,37]. Manoharan et al. further explained various wear mechanism, such as the formation contact plateaus, and fiber-matrix debonding that resulting in fiber pull-out, fracture and damage [37].

Above all, basalt fibers are useful for the preparation of resin-based friction composites as reinforcement components. Our previous work indicated that the physico-chemical characteristics of natural minerals, such as their composition, morphology, structure and thermal stability, had a certain influence on the properties of the prepared composites [38–44]. In this paper, the composition, morphology, functional group, and thermo-stability of basalt fibers are introduced first. Then, based on a newly designed formulation of friction composite, the present work aims to evaluate the potential performance of the composites with different content of basalt fibers. Furthermore, the study is aimed at exploring and analyzing the possible mechanism of interfacial structure between basalt fiber and resin-based friction materials on performance of brake pads.

2. Experimental

2.1. Fabrication of the Friction Materials

Fabrication of the friction materials was based on a typical non-asbestos organic (NAO) type formulation composed of binders (phenolic resin and chemigum), reinforcements (basalt fiber as the studied fiber; aramid pulp, copper fiber and calcium sulfate whisker as the assistance fibers), abrasives (zirconite and friction powder), solid lubricants (synthetic graphite, antimony sulfide and petroleum coke) and fillers (barite) amounting to 100% by weight. In order to study the effect of basalt fiber with different content on the properties of friction materials, the content of basalt fiber was increased by 5%, and the content of barite was decreased at the same time. The compositional variation and the designations for the manufactured composites were summarized in Table 1. Five samples were prepared for each group. All the ingredients of the friction material were provided by the Xi'an Hongqi Brake Factory in China at a commercial grade without further treatment. Basalt is chemically rich with oxides of magnesium, calcium, sodium, potassium, silicon and iron, along with traces of alumina [45]. However, because of the different geographical distribution, the prepared basalt fiber may have a modicum difference in chemical content. According to the result of XRF, the details of the composition of the as-received basalt fiber that cites SiO_2, Al_2O_3, CaO, Fe_2O_3, MgO, Na_2O, K_2O and TiO_2 contents of 33.8%, 21.23%, 16.52%, 10.53%, 7.52%, 3.1%, 2.12%, and 1.59%, respectively. In the present work, non-asbestos organic brake pad materials filled with different content of basalt fibers were manufactured by dry-mixing, hot press molding, and heat treatment. Detailed fabrication conditions of the composites are given in Table 2. All the brake pad materials were cut into a specified size (25 ± 0.2 mm in length and width, 5~7 mm in thickness) for tribological characterizations.

Table 1. Composition of Basalt fiber sliders (wt%).

Sample	Binder	Basalt Fiber	Assistance Fibers	Abrasives	Solid Lubricants	Barite
Bas-0	8	0	33	6	19	34
Bas-5	8	5	33	6	19	29
Bas-10	8	10	33	6	19	24
Bas-15	8	15	33	6	19	19
Bas-20	8	20	33	6	19	14
Bas-25	8	25	33	6	19	9

Table 2. Details of the processing conditions for composite fabrication.

Procedure	Conditions
Mixing	Pre-dispersion of aramid pulps for 10 s, then mixtures of powdery ingredients with pulps and fibers for 10 to 15 s, Chopper RPM: 28,000
Hot press molding	Temperature: 155 ± 5 °C, compression: 5 MPa, curing time: 6 min
Heat treatment	Room temperature to 150 °C, 1 h; constant temperature of 150 °C, 1 h; 150 °C to 160 °C, 1 h; constant temperature of 160 °C, 1.5 h; 160 °C to 170 °C, 1 h; constant temperature of 170 °C, 1.5 h; 170 °C to 180 °C, 1 h; constant temperature of 180 °C, 3 h; 180 °C to room temperature, 1.5 h

2.2. Characterizations of the Basalt Fiber

The chemical constitution of the basalt fiber was analyzed by Bruker S4 Pioneer X-ray fluorescence (XRF) spectrometer (Bruker, Karlsruhe, Germany). The phase composition of the basalt fiber was recorded on a Bruker-AXSD8 Advance Diffractometer (XRD, Bruker, Karlsruhe, Germany) with CuKα radiation (λ = 0.15406 nm) at 40 kV and 40 mA. The scan rate was 0.02 °/s. The morphology of the basalt fiber was observed using a Mira3 LMU field emission scanning electron microscopy (SEM, Tescan, Brno, Czech Republic). The surface functional groups of the basalt fiber were detected by a Tensor II Fourier infrared (FTIR) spectrometer (Bruker, Karlsruhe, Germany) using KBr pellets between 4000 cm^{-1} and 400 cm^{-1}. The thermal performance (thermogravimetry and differential scanning calorimeter, abbreviation for TG-DSC) of the basalt fiber was analyzed using Mettler-Toledo TGA DSC3+ 1600LF thermal analyzer (Mettler-Toledo, Zurich, Switzerland) under air atmosphere with a heating rate of 10 °C/min from room temperature to 800 °C.

2.3. Physical and Mechanical Characterizations of the Composites

Physical properties such as density, hardness, and thermal expansivity of the composites were measured on the basis of Chinese Building Materials Federation Standard JC685-2009, Chinese National Standard GB5766-2007, and GB22310-2008 on a ME104 density balance containing DS1 density components (Mettler-Toledo, Zurich, Switzerland), a XHRD-150 electric plastic rockwell apparatus (Huayin, Laizhou, China), and a XYP-B compression thermal expansion testing machine (Xinyi, Xianyang, China), respectively. The mechanical properties, for instance internal shear strength and compressibility characteristics as a function of content of the basalt fiber, have been determined following Chinese Automobile Industry Standard QC473-1999 and Chinese National Standard GB22311-2008. Internal shear strength was measured on a WDW-50 electronic universal testing machine (Tianchen, Jinan, China) and compressibility test was conducted on a JF221A compressibility machine (Institute of Mechanical and Electrical Equipment, Jilin, China). Fracture surface structure of the composites was observed to reveal the possible reinforcing mechanism by a Nova Nano SEM230 field emission scanning electron microscope (Thermo Fisher, New York, NY, USA).

2.4. Tribological Performance Evaluation of the Composites

A XD-MSM machine (Xinyi, Xianyang, China) was used to investigate the friction performance, and the schematic draft of the tester can be seen from the paper written by Hou et al. [7]. The friction test was performed at temperature range of 100~350 °C with applied normal pressure of 0.98 MPa and speeds in the interval of 7.8 m/s according to Chinese National Standard GB 5763-2008. Two small polished specimens were embedded into the supporting arm and rubbed below 100 °C for a good contact between the small brake pads and dual disc made of grey cast iron. Then, the instant coefficient of friction was recorded on computer and the average friction coefficient was computed automatically during heating process (at 100, 150, 200, 250, 300, and 350 °C) and cooling process (at 300, 250, 200, 150, and 100 °C) separately. The wear rate (the ratio of volume wear loss to frictional work of the lining under specified conditions) of the blocks during the heating process was also measured and calculated. The calculation formula is followed by our previous work [7]. Eleven friction coefficient data and six wear rate data of each friction block were obtained for tribological performance evaluation of the friction composites. The worn surface structure of the composites was observed to reveal the possible tribological mechanism by a Nova Nano SEM230 field emission scanning electron microscope.

3. Results and Discussion

3.1. Phase Composition, Morphology, and Properties of Basalt Fiber

Basalt fiber obtained by melting basalt shows amorphous SiO_2, which was confirmed by widely-angle X-ray diffraction (WAXRD) of the samples (Figure 1a). SEM imaging shows that the average diameter of as-received basalt fiber is roughly 6 μm that measured by a nano measurer according to 100 diameter specimens (Figure 1b). An obvious inhomogeneous distribution in the length of basalt fiber is observed from the microgram, which is related to our choice of cheap commercial basalt fibers. On account of its length-diameter ratio, the as-received studied fiber should be viewed as chopped basalt fibers with unique strengthen strategies. Figure 1c represents the characteristic peaks of the as-received basalt fiber. The peaks at 3423 cm^{-1} and 1641 cm^{-1} result from stretching vibration and bending vibration of liquid water molecules that adsorbed on the silica forms respectively [46]. The strongest band at 997 cm^{-1} is ascribed to the stretching vibration of the Si−O bond. Si−O bond also gives a weak characteristic peak due to bending vibration at 729 cm^{-1}. The peak appeared at 489 cm^{-1} may be caused by vibration of Mg−O and Al−O. FTIR analysis verifies that basalt fiber is combined to covalent bond and ionic bond with higher temperature resistance. Thermal decomposition property of basalt fiber was investigated using a simultaneous thermal analyzer (Figure 1d). The only apparent weight loss of 5.03 wt% was detected between 200 °C to 550 °C with an endothermal peak of around 430 °C, which should be attributed to the removal of crystal water. Although there is a little crystal water lost, the basalt fiber has an excellent performance in terms of heat resistance. According to the composition, morphology, bonding, and thermal properties, basalt fiber exhibits outstanding thermostability with enhancement effect.

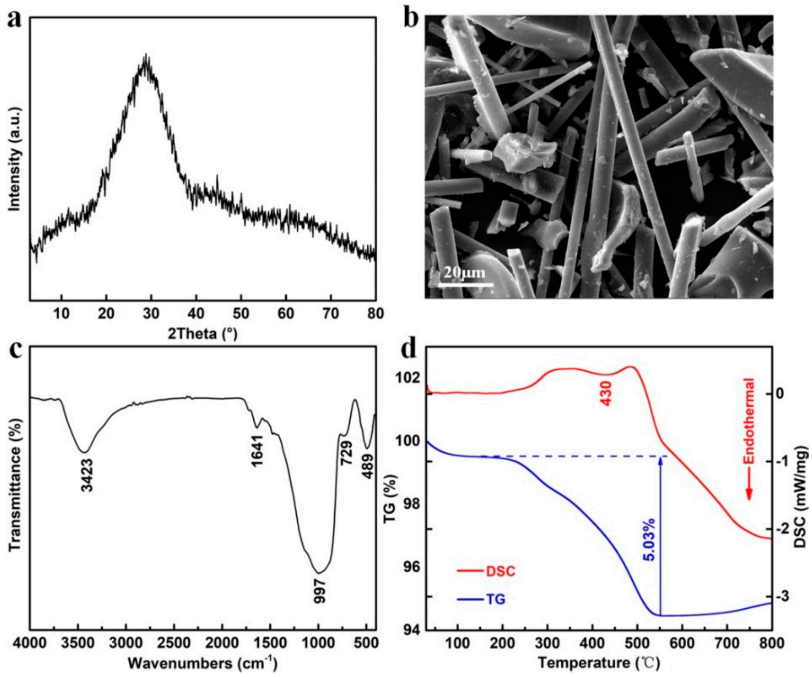

Figure 1. (**a**) XRD pattern, (**b**) SEM image, (**c**) FTIR spectrum, and (**d**) TG and DSC curves of basalt fiber.

3.2. Effect of Basalt Fiber Content on the Properties of Composites

Various physical and mechanical properties of the friction composites were characterized shown in Table 3, Figures 2 and 3. In the case of the density of brake pad, it will affect the weight of an automobile. As evident from Table 3, the density of the samples added in basalt fiber increases compared to the sample without basalt fiber. Moreover, with the increase of basalt fiber content, the density increases and culminates when basalt fiber content reaches at 15%, then begins to decrease. The increase in the density of the brake pad is bad for business application, since greater density will increase the weight of a car. However, the increase of density in this work is well within the permissible limit of Chinese National Standard. Hardness shows a tendency to rise and then fall, and culminates at a fiber content of 20% (except for the sample with 10% fiber content, which possibly caused by uneven mixing). For the automobile brake pad, the appropriate rockwell hardness ranges from 40 to 90 HRM. It can be seen from Table 3 that all samples are within this range, in addition to the sample with 10% fiber content. Among these samples, the sample with fiber content of 15% can be regard as the most appropriate hardness. The thermal expansion is another important parameter for evaluating a brake pad, which is connected with the frictional undulation. According to the requirement of Chinese National Standard, the coefficient of thermal expansion shouldn't exceed 2.5% at the measuring temperature of about 400 °C. As shown in Table 3, the coefficient of thermal expansion shows a similar variation trend to the hardness, and all the samples accord with the requirement of Chinese National Standard except for the sample with 20% fiber content.

Table 3. Physical properties of the composites.

Content of Basalt Fiber (wt%)	0	5	10	15	20	25
Density (g/cm^3)	1.94	2.00	2.16	2.29	2.27	1.99
Rockwell hardness (HRM)	45.4	46	27.4	68	75	41.6
Thermal expansion coefficient (%)	1.34	1.73	1.95	2.10	2.85	2.06

The friction composite is required with sufficient mechanical strength to ensure that there is no damage or breakage in the process of processing or braking application. Internal shear strength and compression strain of friction composites are important properties to measure the emergency braking ability of automobile braking system. The variations in internal shear strength and compression strain as a function of their composition such as basalt fiber content are shown in Figures 2 and 3. Internal shear strength is the ratio of shear force to shear area. From the perspective of the whole variation range given in Figure 2, the internal shear strength of the friction composites increases first and then decreases with the increase of basalt fiber content, and reaches the maximum when the fiber content reaches at 15%. Actually, the basalt fibers, as a supporting material in the friction material, provide sufficient mechanical strength for the friction products to resist load force (such as: impact force, internal shear force, and pressure). If the fiber content is too low, the load is difficult to uniformly distribute to more fibers, while too much fiber will obviously increase the fracture. According to enterprise standards JF04-2A 1996, the value of internal shear strength is required to be no less than 11.8 MPa, which surpasses that of Chinese National Standard (no less than 2.5 MPa). In spite of this, all the samples are well within the permissible limit of Chinese National Standard, and the sample with fiber content of 15% is able to adapt to more stringent braking environment. The compression strain is the ratio of the thickness reduction of the brake lining caused by pressure and temperature to the initial thickness. On the basis of Chinese National Standard, the compression strain should be inferior to 2% at room temperature and 5% at 400 °C. As is shown in Figure 3, the compression strain of the samples all meets this requirement. With the increase of fiber content, the compression strain at room temperature decreases first and then increases again (Figure 3a), while that at 400 °C decreases all along (Figure 3b). The smaller the compression strain, the less the sample is affected by temperature and pressure. Obviously, the addition of basalt fiber could improve the mechanical properties of the friction composites significantly. In comparison, the sample with fiber content of 15% exhibits the highest internal shear strength, suitable hardness, and lower compression strain, thermal expansion coefficient and density, indicating that the composite is more appropriate as a brake lining.

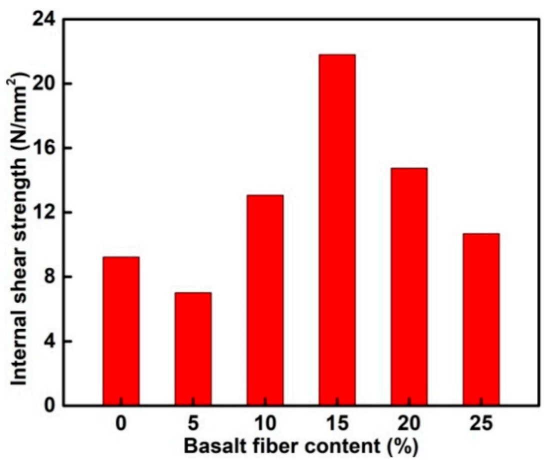

Figure 2. Internal shear strength of the friction composites.

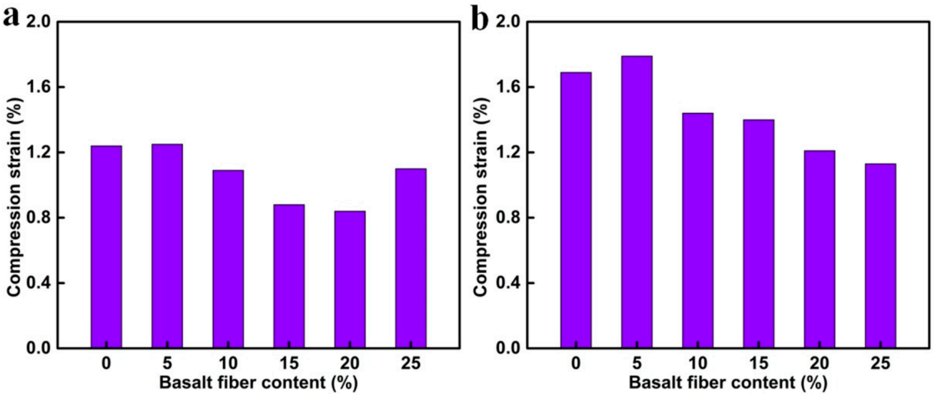

Figure 3. Compression strain of the friction composites: (**a**) at room temperature and (**b**) at the temperature of 400 °C.

3.3. Fracture Surface Analysis

The mechanical properties of the friction composites Bas-0, Bas-5, Bas-15 and Bas-25 are affected by the interfacial microstructure between basalt fibers and resin-based matrix. SEM images of fracture surface of the friction composites are shown in Figure 4, and it can be seen that rigid basalt fibers randomly distributed in the matrix work as supporting framework as indicated by the arrows. If the fiber content (Figure 4a,b) is lower than the optimal value (Figure 4c), load could not be uniformly distributed to more fibers, which are not well bonded with the resin and fiber, resulting in the decline of the mechanical properties of the friction composites. The fracture mechanism has shown that the fracture starts from the end of the fiber and spreads along the interface between the fiber and the matrix under load [35]. When the fiber content is higher than the optimal value, the fiber fracture increases (as indicated by the ellipse shown in Figure 4d), which also results in the decrease of the mechanical properties of the friction composites. According to the results detailed above, it is further revealed that the friction composite with 15% of basalt fiber is deemed to have the best comprehensive mechanical performance.

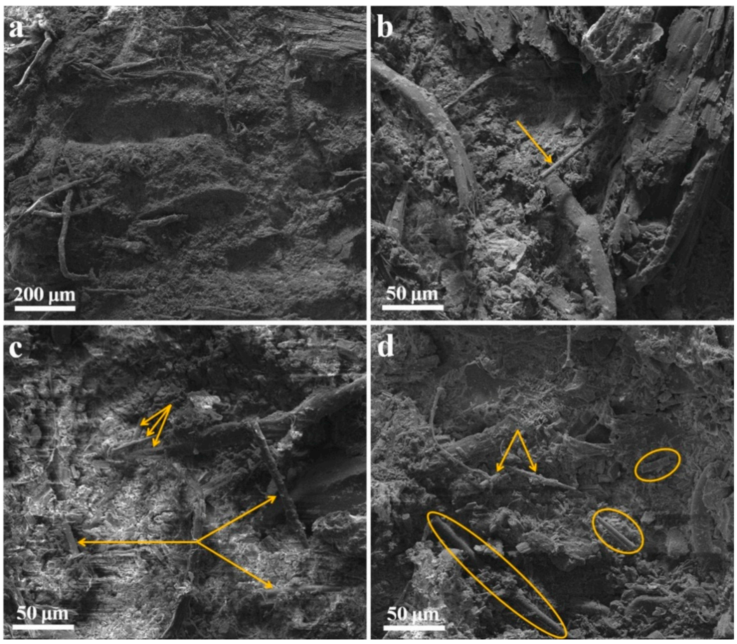

Figure 4. SEM images of the fracture surface of the friction composites: (**a**) Bas-0; (**b**) Bas-5; (**c**) Bas-15; and (**d**) Bas-25. Arrows indicate the reinforcing fibers, and ellipses indicate the broken fibers.

3.4. Effect of Basalt Fiber Content and Temperature on Tribology Performance

Details of basalt fiber content and temperature on the friction coefficient of the composites were discussed in Figure 5a,b. The relationships among coefficient of friction, composition, and temperature are non-liner. The influence of temperature on friction coefficient is complex, but it is mainly manifested that the friction coefficient increases with the increase of temperature and culminates at 300 °C, then begins to decrease. It is evident that the friction coefficient increases with the increase of fiber content during heating process (apart from the broken line without basalt fiber), and culminates at 20% of basalt fiber, then begins to decrease (Figure 5a). During the cooling process shown in Figure 5b, the coefficient of friction behaves with a similar trend to the heating process at basalt fiber content higher than 10%. Öztürk et al. thought the increase in friction coefficient with increasing basalt fiber content was related to the addition of this hard fiber enhancing the ploughing action of surface of the friction composites on surface of the metallic disc [47]. However, when the content of basalt fiber was too high, the surface integrity of friction composites became worse, resulting in the decrease of friction coefficient. In a word, the effect of basalt fiber content on friction coefficient is obvious and the fade of friction coefficient appears at higher content of basalt fiber and higher temperature.

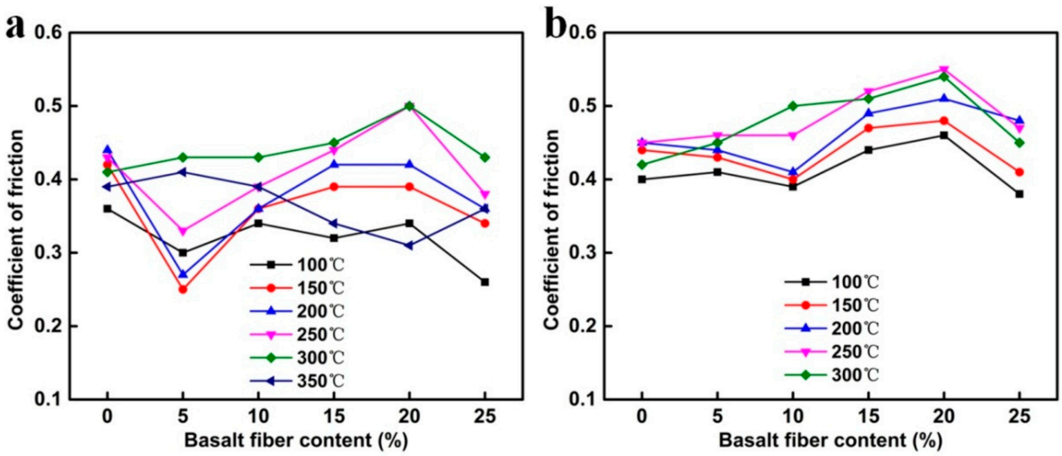

Figure 5. Effects of basalt fiber content on coefficient of friction in (**a**) heating processing and (**b**) cooling processing at different temperatures.

Drivers prefer expecting a smooth braking at unpredictable diverse braking conditions in brake applications, so it is important for friction material manufacture to produce commercial brake pads with friction stability. Extension evaluation [48,49] based on extenics theory was developed to evaluate the relationships between coefficient of friction of the friction composites and basalt fiber content for obtaining better friction stability formula. According to the reports [3], the procedures of the extension evaluation areas follow. Assuming that there is an interval $X = \langle a,b \rangle$ and a point $M \in X$, the dependent degree function of any point $x \in -\infty,+\infty$ with respect to the interval X and the point M is defined by Equation (1):

$$\mathrm{K}(x) = \begin{cases} \frac{x-a}{M-a}, & x \le M \\ \frac{b-x}{b-M}, & x \ge M \end{cases} \quad (1)$$

For the coefficient of friction (μ), let $M = (a + b)/2$ (assuming that the best coefficient of friction is the middle point of interval X on the basis the brake linings Chinese National Standard GB 5763-2008 shown in Table 4), the dependent degree function is changed into Equation (2):

$$\mathrm{K}(\mu_i) = \begin{cases} \frac{2(\mu_i - a_i)}{b_i - a_i}, & \mu_i \le \frac{a_i + b_i}{2} \\ \frac{2(b_i - \mu_i)}{b_i - a_i}, & \mu_i \ge \frac{a_i + b_i}{2} \end{cases} \quad (2)$$

The dependent degree $K(x_i)$ was calculated at each temperature in heating and cooling process, and each of the eleven measured coefficient of friction has equal importance to this evaluation, with a same weight (α_i) described by Equation (3). $\overline{K_\mu(x)}$, the weighted average dependent degree can be used to compare and rank different samples, and the higher the value of $\overline{K_\mu(x)}$, the better friction stability is.

$$\overline{K_\mu(x)} = \sum_{i=1}^{11} \alpha_i K(\mu_i),\ \alpha_1 = \alpha_2 = \ldots = \alpha_{11} = \frac{1}{11} \tag{3}$$

The greater the $\overline{K_\mu(x)}$ value, the more stable the friction coefficient of the brake block, and the closer the dependent degree is to 1, the better the evaluation result is. The results of extension evaluation on relationships between friction coefficient and content of fibers by Equation (3) are shown in Table 5. Without considering physical and mechanical properties of the friction composites, the samples ranked from best to worst are Bas-0, Bas-15, Bas-20, Bas-10, Bas-25, and Bas-5. The samples Bas-0 and Bas-15 have similar frictional stability, which belongs to the optimal level.

Wear in terms of wear rate, total wear rate and total weight loss was observed in all the friction composites (Figure 6). All wear rate values are far less than the requirements of GB 5763-2008 listed in Table 5. It exhibits also non-linear relationship among the wear rate, composition, and temperature (Figure 6a). When the fiber content is too high (20% and 25%) or too low (0%), the value and fluctuation of wear rate are both high with the temperature changes. The variation of wear rate with temperature follows the trend: higher temperature induces high wear, which could be mainly due to that the friction composites may be largely thermally activated [50]. Kim et al. indicated that the improvements or deterioration in wear performance of friction composites was depended on the thermal stability of rein binder [51]. With the increase of temperature to a certain value, organic binders such as resins begin to soften, and even decompose thermally, leading to weaker bonds among binders, fibers, and other fillers, finally the wear increased. The samples with 5%, 10%, and 15% of fiber contents were observed relatively stable, and had low wear rate with the temperature changes, because suitable basalt fiber can improve the integrality of the friction composite, which has a positive effect on stabilizing and decreasing the wear rate. Figure 6b shows the variations of total wear rate and total weight loss of the friction composites with basalt fiber content. With the increase of basalt fiber content, the total wear rate decreases first and then increases, whereas the total weight loss increases all through. When content of basalt fiber exceeds 20%, the surface of friction material was badly worn. A comprehensive comparison of the total wear rate and the total weight loss shows the optimal formulation of these samples is Bas-15.

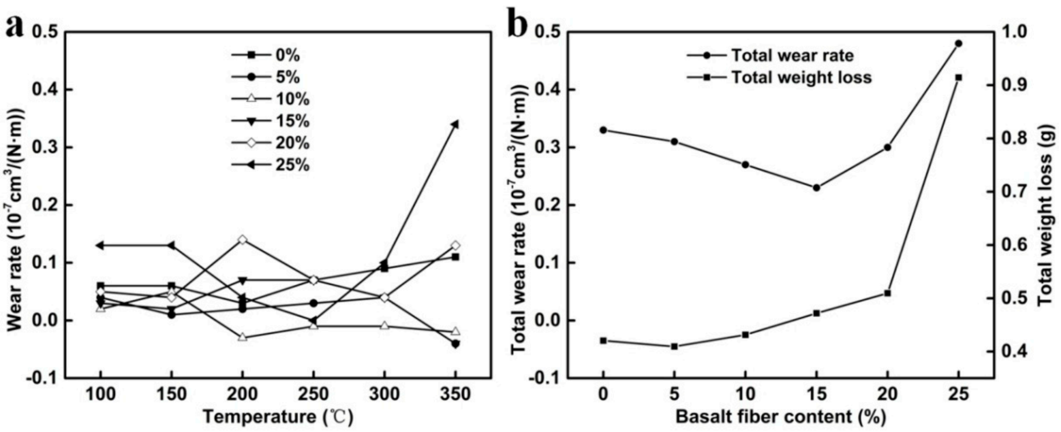

Figure 6. (**a**) Variations of wear rate of the friction composites with basalt fiber content and temperature; (**b**) Variations of total weight loss and total wear rate of the friction composites with basalt fiber content.

Table 4. Values of friction properties specified in GB 5763-2008.

Temperature (°C)	100	150	200	250	300	350
μ	0.25–0.65	0.25–0.70	0.25–0.70	0.25–0.70	0.25–0.70	0.25–0.70
$V/10^{-7}cm^3\cdot(Nm)^{-1}$	≤0.50	≤0.70	≤1.00	≤1.50	≤2.00	≤2.50

Table 5. Results of friction coefficient by extension evaluation method.

Parameters	Bas-0	Bas-5	Bas-10	Bas-15	Bas-20	Bas-25
$\overline{K_\mu(x)}$	0.765	0.588	0.670	0.761	0.738	0.637
Rank (μ)	1	6	4	2	3	5

3.5. Worn Surface Analysis

Many friction characteristics between NAO friction materials and cast iron discs can be explained by the formation of contact plateaus. The worn surfaces of the friction composites Bas-0, Bas-5, Bas-15 and Bas-25 were observed as shown in Figure 7. According to Figure 7a,c, the worn surface micrographs of Bas-0 and Bas-15 are mainly consisting of primary contact plateaus, which formed due to the lower removal rate of the fibers/wear resistant ingredients. The increase of tribology performances in the friction process is mainly related to the formation of the primary contact plateaus. When the primary contact plateaus form, the real contact area between brake pad and disc is increased, and further result in an increased coefficient of friction. The formation of the primary contact plateau also means that the surfaces of the brake pad are worn smooth, giving rise to the stability of the friction properties. However, in case of the friction composites Bas-5 (Figure 7b) and Bas-25 (Figure 7d), the wear surface morphology also appears secondary contact plateaus apart from primary contact plateaus. The secondary contact plateaus are formed by compaction of the debris under load, shear force and friction heat. It is easily observed that secondary contact plateaus are loosely adhered to the underneath subsurface. These secondary contact plateaus are likely to be damaged at the next braking process, resulting in increased friction fluctuations and severe wear. According to previous work [52], the abrasives and solid lubricants play a crucial part in improving and stabilizing coefficient of friction and decreasing wear in the friction composite. However, suitable fiber content is also helpful to improve the integrity of the composite, which can prevent the fillers (abrasives, solid lubricants, functional fillers, and space fillers) from dislodging easily. In this work, the combination of fiber-fillers/resin was enhanced when basalt fiber content was 15%, which further caused the friction composite to behave well.

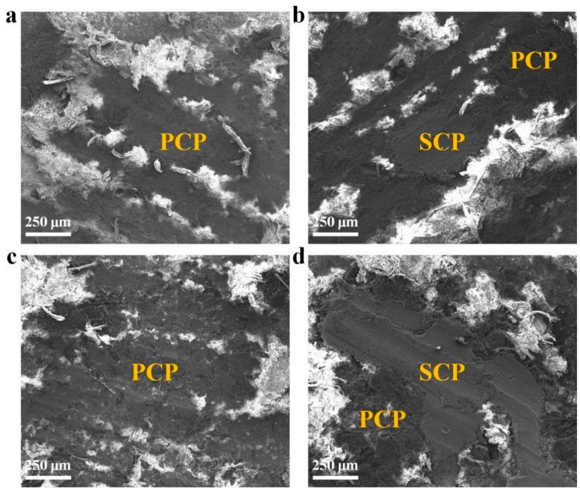

Figure 7. SEM images of the worn surface of the friction composites: (**a**) Bas-0; (**b**) Bas-5; (**c**) Bas-15; and (**d**) Bas-25. PCP indicates primary contact plateaus and SCP indicates secondary contact plateaus.

4. Conclusions

The physico-mechanical and tribological performance of the friction composites based on atypical non-asbestos organic (NAO) type formulation containing different contents of basalt fibers has been evaluated. The mechanical properties of the friction composites were improved due to the basalt fiber added. Too high or too low contents of basalt fiber were unfavorable to the mechanical properties of the friction composites. The best mechanical behavior was obtained in Bas-15 composite. The probable mechanism may be that thousands of basalt fibers were dispersed into resin-based brake composites, behaved as nets and skeletons, which strengthened the brake composites effectively. From the tribology tests, the coefficient of friction and wear rate values all met the requirements of GB 5763-1998. The relationships among coefficient of friction, composition, and temperature are non-linear. Extension evaluation based on extenics theory was developed to evaluate the non-linear relationships, and the results showed that the samples Bas-0 and Bas-15 had similar frictional stability, which belonged to the optimal level. It showed also non-linear relationships among the wear rate, composition, and temperature. A comprehensive comparison of the total wear rate and the total weight loss demonstrates the sample Bas-15 was the optimal formulation. The worn surface analysis indicated that the worn surfaces had revealed two kinds of contact plateaus, namely primary contact plateaus and secondary contact plateaus. The former could provide a higher and stable friction coefficient, while the latter was prone to serious friction fluctuations and wear. The abrasives and solid lubricants played an important part in regulating the two kinds of contact plateau. When basalt fiber content was 15%, the integrity of the fiber-fillers/resin was enhanced, which helped the friction composite to behave well.

Author Contributions: H.Y. (conceiving the project and writing the final paper). X.Z. (writing initial drafts of the work). X.Z. and J.O. (designing and performing the experiments, characterizing the materials, and analyzing the data). Q.T. (giving expert comments on the manuscript and participating in the discussion). All authors have read and agreed to the published version of the manuscript.

Funding: This work was financially supported by the National Key R&D Program of China (2017YFB0310903), the Hunan Provincial Science and Technology Project (and 2018WK4023), and the Hunan Provincial Co-Innovation Centre for Clean and Efficient Utilization of Strategic Metal Mineral Resources (2014-405).

Conflicts of Interest: The authors declare no conflict of interest.

References

1. Liew, K.W.; Nirmal, U. Frictional performance evaluation of newly designed brake pad materials. *Mater. Des.* **2013**, *48*, 25–33. [CrossRef]
2. Dennis, J.P.; Brent, L.F.; Elizabeth, T.L.; Gregory, P.B.; Patrick, J.S. Environmental and occupational health hazards associated with the presence of asbestos in brake linings and pads (1900 to present): A "state-of-the-art" review. *J. Toxicol. Environ. Health B* **2004**, *7*, 25–80.
3. Fu, Z.Z.; Suo, B.T.; Yun, R.P.; Lu, Y.M.; Wang, H.; Qi, S.C.; Jiang, S.G.; Lu, Y.F. Development of eco-friendly brake friction composites containing flax fibers. *J. Reinf. Plast. Comp.* **2012**, *31*, 681–689. [CrossRef]
4. Singh, T.; Patnaik, A.; Chauhan, R.; Rishiraj, A. Assessment of braking performance of lapinus-wollastonite fibre reinforced friction composite materials. *J. King Saud Univ.-Eng. Sci.* **2017**, *29*, 183–190. [CrossRef]
5. Tong, J.; Ma, Y.H.; Jiang, M. Effects of the wollastonite fiber modification on the sliding wear behavior of the UHMWPE composites. *Wear* **2003**, *255*, 734–741. [CrossRef]
6. Tej, S.; Avinash, T.; Amar, P.; Ranchan, C.; Sharafat, A. Influence of wollastonite shape and amount on tribo-performance of non-asbestos organic brake friction composites. *Wear* **2017**, *386–387*, 157–164.
7. Hou, K.; Ouyang, J.; Zheng, C.H.; Zhang, J.H.; Yang, H.M. Surface-modified sepiolite fibers for reinforcing resin brake composites. *Mater. Express* **2017**, *7*, 104–112. [CrossRef]
8. Kuroe, M.; Tsunoda, T.; Kawano, Y.; Takahashi, A. Application of lignin-modified phenolic resins to brake friction material. *J. Appl. Polym. Sci.* **2013**, *129*, 310–315. [CrossRef]
9. Bernard, S.S.; Jayakumari, L.S. Pressure and temperature sensitivity analysis of palm fiber as a biobased reinforcement material in brake pad. *J. Braz. Soc. Mech. Sci.* **2018**, *40*, 152. [CrossRef]

10. Ikpambese, K.K.; Gundu, D.T.; Tuleun, L.T. Evaluation of palm kernel fibers (PKFs) for production of asbestos-free automotive brake pads. *J. King Saud Univ. Eng. Sci.* **2016**, *8*, 110–118. [CrossRef]
11. Ma, Y.H.; Wu, S.Y.; Tong, J.; Zhao, X.L.; Zhuang, J.; Liu, Y.C.; Qi, H.Y. Tribological and mechanical behaviours of rattan-fibre-reinforced friction materials under dry sliding conditions. *Mater. Res Express* **2018**, *5*, 035101. [CrossRef]
12. Aranganathan, N.; Mahale, V.; Bijwe, J. Effects of aramid fiber concentration on the friction and wear characteristics of non-asbestos organic friction composites using standardized braking tests. *Wear* **2016**, *354–355*, 69–77. [CrossRef]
13. Kim, S.H.; Jang, H. Friction and vibration of brake friction materials reinforced with chopped glass fibers. *Tribol. Lett.* **2013**, *52*, 341–349. [CrossRef]
14. Baklouti, M.; Cristol, A.L.; Desplanques, Y.; Elleuch, R. Impact of the glass fibers addition on tribological behavior and braking performances of organic matrix composites for brake lining. *Wear* **2015**, *330–331*, 507–514. [CrossRef]
15. Sahin, Y.; Baets, P.D. Friction and wear behavior of carbon fabric-reinforced epoxy composites. *JOM J. Miner. Met. Mater. Soc.* **2017**, *69*, 2443–2447. [CrossRef]
16. Guo, W.J.; Bai, S.X.; Ye, Y.C.; Zhu, L.A.; Li, S. A new strategy for high-value reutilization of recycled carbon fiber: Preparation and friction performance of recycled carbon fiber felt-based C/C-SiC brake pads. *Ceram. Int.* **2019**, *45*, 16545–16553. [CrossRef]
17. Ilanko, A.K.; Vijayaraghavan, S. Wear behavior of asbestos-free eco-friendly composites for automobile brake materials. *Friction* **2016**, *4*, 144–152. [CrossRef]
18. Colombo, C.; Vergani, L.; Burman, M. Static and fatigue characterization of new basalt fibre reinforced composites. *Compos. Struct.* **2012**, *94*, 1165–1174. [CrossRef]
19. Pavlovski, D.; Mislavsky, B.; Antonov, A. CNG cylinder manufacturers test basalt fibre. *J. Reinf. Plast. Comp.* **2007**, *51*, 36–39. [CrossRef]
20. Dehkordi, M.T.; Nosraty, H.; Shokrieh, M.M.; Minak, G.; Ghelli, D. The influence of hybridization on impact damage behavior and residual compression strength of intraply basalt/nylon hybrid composites. *Mater. Des.* **2013**, *43*, 283–290. [CrossRef]
21. Branston, J.; Das, S.; Kenno, S.Y.; Taylor, C. Mechanical behaviour of basalt fibre reinforced concrete. *Constr. Build. Mater.* **2016**, *124*, 878–886. [CrossRef]
22. Kabay, N. Abrasion resistance and fracture energy of concretes with basalt fiber. *Constr. Build. Mater.* **2014**, *50*, 95–101. [CrossRef]
23. Sim, J.; Park, C.; Moon, D.Y. Characteristics of basalt fiber as a strengthening material for concrete structures. *Compos. Part B Eng.* **2005**, *36*, 504–512. [CrossRef]
24. Kim, M.T.; Kim, M.H.; Rhee, K.Y.; Park, S.J. Study on an oxygen plasma treatment of a basalt fiber and its effect on the interlaminar fracture property of basalt/epoxy woven composites. *Compos. Part B Eng.* **2011**, *42*, 499–504. [CrossRef]
25. Lee, S.O.; Rhee, K.Y.; Park, S.J. Influence of chemical surface treatment of basalt fibers on interlaminar shear strength and fracture toughness of epoxy-based composites. *J. Ind. Eng. Chem.* **2015**, *32*, 153–156. [CrossRef]
26. Lopresto, V.; Leone, C.; Iorio, I.D. Mechanical characterisation of basalt fibre reinforced plastic. *Compos. Part B Eng.* **2011**, *42*, 717–723. [CrossRef]
27. Fiore, V.; Bella, G.D.; Valenza, A. Glass-basalt/epoxy hybrid composites for marine applications. *Mater. Des.* **2011**, *32*, 2091–2099. [CrossRef]
28. Wang, X.; Wu, G.; Wu, Z.S.; Dong, Z.Q.; Xie, Q. Evaluation of prestressed basalt fiber and hybrid fiber reinforced polymer tendons under marine environment. *Mater. Des.* **2014**, *64*, 721–728. [CrossRef]
29. Shi, J.Z.; Wang, X.; Wu, Z.S.; Zhu, Z.G. Fatigue behavior of basalt fiber-reinforced polymer tendons under a marine environment. *Constr. Build. Mater.* **2017**, *137*, 46–54. [CrossRef]
30. Dehkordi, M.T.; Nosraty, H.; Shokrieh, M.M.; Minak, G.; Ghelli, D. Low velocity impact properties of intra-ply hybrid composites based on basalt and nylon woven fabrics. *Mater. Des.* **2010**, *31*, 3835–3844. [CrossRef]
31. Eslami-Farsani, R.; Khalili, S.M.R.; Hedayatnasab, Z.; Soleimani, N. Influence of thermal conditions on the tensile properties of basalt fiber reinforced polypropylene-clay nanocomposites. *Mater. Des.* **2014**, *53*, 540–549. [CrossRef]
32. Li, X.; Yahya, M.Y.; Nia, A.B.; Wang, Z.H.; Yang, J.L.; Lu, G.X. Dynamic failure of basalt/epoxy laminates under blast-Experimental observation. *Int. J. Impact Eng.* **2017**, *102*, 16–26. [CrossRef]

33. Peng, Y.; Wu, H.; Fang, Q.; Liu, J.Z.; Gong, Z.M. Impact resistance of basalt aggregated UHP-SFRC/fabric composite panel against small caliber arm. *Int. J. Impact Eng.* **2016**, *88*, 201–213. [CrossRef]
34. Thirumalai, R.; Prakash, R.; Ragunath, R.; SenthilKumar, K.M. Experimental investigation of mechanical properties of epoxy based composites. *Mater. Res. Express* **2019**, *6*, 075309. [CrossRef]
35. Amuthakkannan, P.; Manikandan, V.; Winowlin Jappes, J.T.; Uthayakumar, M. Effect of fibre length and fibre content on mechanical properties of short basalt fibre reinforced polymer matrix composites. *Mater. Phys. Mech.* **2013**, *16*, 107–117.
36. Ilanko, A.K.; Vijayaraghavan, S. Wear mechanism of flax/basalt fiber-reinforced eco-friendly brake friction materials. *Tribol. Mater. Surf. Interfaces* **2017**, *11*, 47–53. [CrossRef]
37. Manoharan, S.; Vijay, R.; Lenin Singaravelu, D.; Krishnaraj, S.; Suresha, B. Tribological characterization of recycled basalt-aramid fiber reinforced hybrid friction composites using grey-based taguchi approach. *Mater. Res. Express* **2019**, *6*, 065301. [CrossRef]
38. Yan, Z.; Fu, L.; Zuo, X.; Yang, H. Green assembly of stable and uniform silver nanoparticles on 2D silica nanosheets for catalytic reduction of 4-nitrophenol. *Appl. Catal. B Environ.* **2018**, *226*, 23–30. [CrossRef]
39. Peng, K.; Fu, L.; Li, X.; Ouyang, J.; Yang, H. Stearic acid modified montmorillonite as emerging microcapsules for thermal energy storage. *Appl. Clay Sci.* **2017**, *138*, 100–106. [CrossRef]
40. Li, X.; Yang, Q.; Ouyang, J.; Yang, H.; Chang, S. Chitosan modified halloysite nanotubes as emerging porous microspheres for drug carrier. *Appl. Clay Sci.* **2016**, *126*, 306–312. [CrossRef]
41. Zhang, Y.; Tang, A.; Yang, H.; Ouyang, J. Applications and interfaces of halloysite nanocomposites. *Appl. Clay Sci.* **2016**, *119*, 8–17. [CrossRef]
42. Shu, Z.; Zhang, Y.; Yang, Q.; Yang, H. Halloysite nanotubes supported Ag and ZnO nanoparticles with synergistically enhanced antibacterial activity. *Nanoscale Res. Lett.* **2017**, *12*, 135. [CrossRef] [PubMed]
43. Peng, K.; Fu, L.; Ouyang, J.; Yang, H. Emerging parallel dual 2D composites: Natural clay mineral hybridizing MoS_2 and interfacial structure. *Adv. Funct. Mater.* **2016**, *26*, 2666–2675. [CrossRef]
44. Niu, M.; Yang, H.; Zhang, X.; Wang, Y.; Tang, A. Amine-impregnated mesoporous silica nanotube as an emerging nanocomposite for CO_2 Capture. *ACS Appl. Mater. Interfaces* **2016**, *8*, 17312–17320. [CrossRef] [PubMed]
45. Dhand, V.; Mittal, G.; Rhee, K.Y.; Park, S.J.; Hui, D. A short review on basalt fiber reinforced polymer composites. *Compos. Part B Eng.* **2015**, *73*, 166–180. [CrossRef]
46. Yassien, K.M.; El-Bakary, M.A. Effect of gamma irradiation on the physical and structural properties of basalt fiber. *Microsc. Res. Tech.* **2019**, *82*, 643–650. [CrossRef]
47. Özturk, B.; Arslan, F.; Özturk, S. Effects of different kinds of fibers on mechanical and tribological properties of brake friction materials. *Tribol. Trans.* **2013**, *56*, 536–545. [CrossRef]
48. Yun, R.P.; Lu, Y.F.; Filip, P. Application of extension evaluation method in development of novel eco-friendly brake material. *SAE Int. J. Mater. Manuf.* **2010**, *2*, 1–7. [CrossRef]
49. Yun, R.P.; Martynkova, S.G.; Lu, Y.F. Performance and evaluation of nonasbestos organic brake friction composites with SiC particles as an abrasive. *J. Compos. Mater.* **2011**, *45*, 1585–1593.
50. Dadkar, N.; Tomar, B.S.; Satapathy, B.K.; Patnaik, A. Performance assessment of hybrid composite friction materials based on flyash-rock fibre combination. *Mater. Des.* **2010**, *31*, 723–731. [CrossRef]
51. Kim, S.J.; Jang, H. Friction and wear of friction materials containing two different phenolic resins reinforced with aramid pulp. *Tribol. Int.* **2000**, *33*, 477–484. [CrossRef]
52. Zhao, X.; Ouyang, J.; Tan, Q.; Tan, X.; Yang, H. Interfacial characteristics between mineral fillers and phenolic resin in friction materials. *Mater. Express* **2020**, *10*, 70–80. [CrossRef]